

Low-energy ball-milling: Transformations of boron nitride powders. Crystallographic and chemical characterizations

M. GASGNIER

Laboratoire de Chimie Inorganique, ICMO, UMR 8613 du CNRS, Bâtiment 420, Université Paris Sud, 91504 Orsay, France

H. SZWARC, A. RONEZ

Laboratoire de Chimie Physique des Matériaux Amorphes, UMR 8611 du CNRS, Bâtiment 490, Université Paris Sud, 91504 Orsay, France
E-mail: szwarc@cpma.u-psud.fr

BN powders (with and without water) which have undergone low-energy ball-milling have been studied through X-ray diffraction, transmission electron microscopy, granulometry, electron energy loss (EELS) and IR spectroscopies. The main result is the formation of the orthorhombic and cubic high pressure phases of BN. A “turbostratic” behaviour of hexagonal BN has also been observed. As expected, the grain sizes decrease markedly. It is to be noticed that the presence of water induces some chemical reactions which are revealed through ammonia-like and nitride compounds scents. However, according to EELS measurements, the main transformations are structural ones. © 2000 Kluwer Academic Publishers

1. Introduction

The purpose of the present work was to investigate the possible phase transformations of pure BN under the influence of low-energy ball-milling because ball-milling can induce the formation of high pressure phase modifications. As a matter of fact, it was wondered whether it could directly induce, at room temperature, the formation of cubic BN, the well-known diamond-like high pressure phase, instead of only facilitating its synthesis by submitting ball-milled BN to high temperature-high pressure treatments, as Horiuchi *et al.* did [1].

More than 150 years ago Balmain [2] discovered boron nitride. According to the Chemical Abstracts, the first preparations corresponding to appreciable yields of pure BN were performed in 1908 by Stock and Holle [3]. The role of water as a catalyst for the hexagonal (h-BN) → face-centered cubic (c-BN) high pressure phase transition was recognized [4]. As a matter of fact, the amount of water retained as moisture on dry BN powder seems to be sufficient to diminish the transformation pressure from 100 to 55 kbars.

As to the effect of mechanical stresses on BN, shock-wave compression performed through explosion of a cylindrical charge increases the degree of crystallinity of BN and generate a new crystalline modification, E-BN, whose structure has not been elucidated [5].

Table I summarizes the crystallographic data corresponding to phases formed through high pressure and stress experiments [5–10]. It can be seen that the unit cell parameters are often related through simple ratios,

such as:

$$\begin{aligned} a &= a_h = a_w = a_{rh} = b_m \\ a &= \frac{a_c}{\sqrt{2}} \\ c_{rh} &= 1.5c_h = 4a_{rh} \\ a_o &\sim 2c_w, \quad c_o = \sqrt{3}a_c \\ a_m &\sim c_w, \quad c_m = \frac{c_h}{2} \end{aligned}$$

Therefore, these lattices have common reticular planes [such as: $(220)_{c\text{-BN}} = (11.0)_{h\text{-BN}} = (11.0)_{w\text{-BN}} = (11.0)_{rh\text{-BN}}$ and may easily grow epitaxially. They represent then polytypical phases as was suggested by Horiuchi *et al.* [10]. To that effect, phases c-BN, h-BN, rh-BN, and w-BN may be named 3C, 2H, 3R, and 2H, respectively, according to the polytypism naming [11].

2. Experimental

In our experiments BN powders from two different sources (Aldrich, Grepsy) were studied by low-energy ball-milling [12]. The Aldrich product (called hereafter product A) is pure white and is very fluid. The Grepsy one (that we will call B) is yellowish and coarse-grained. It was previously used for high pressure experiments (~0.5 GPa) as a pressure transmitting material. The characteristics of powders A and B before and after milling are recorded in Table IV.

TABLE I Known crystalline structures of BN

| BN-type | $a/\text{\AA}$ | $b/\text{\AA}$ | $c/\text{\AA}$ | β | Remarks |
|------------------------------|-----------------------------------|--------------------|--|---------|---------------------------|
| h-BN hexagonal (5) | 2.505 | 2.505 | 6.655 | | atmospheric pressure |
| c-BN cubic (6) | 3.615 ($a_h \times 2^{1/2}$) | 3.615 | 3.615 | | 1500 K- 16 GPa |
| w-wurtzite hexagonal (7) | 2.555 (a_h) | 2.555 (a_h) | 4.23 ($a_h \times 3^{1/2}$) | | 55 GPa |
| rh-BN rhombohedral (8) | 2.505 (a_h) | 2.505 (a_h) | 10.010 ($c_h \times 1.5$) ($a_h \times 4$) | | metastable |
| o-BN orthorhombic (4) | 8.600 | 7.740 | 6.350 ($a_c \times 3^{1/2}$) | | shock-wave compression |
| m-BN monoclinic (9) | 4.33 ($a_h \times 3^{1/2}$) | 2.50 (a_h) | 3.25 ($c_h/2$) | 94° | 2100 K- 7.7 GPa |

Note: $d_{11,0}(h) = d_{220}(c) = d_{11,0}(w) = d_{11,0}(r)$.

Powdered samples were introduced into cylindrical steel containers (8 cm deep, 4 cm inner diameter) with a polished hemispherical bottom containing 20 stainless steel balls (2 g, 0.8 cm diameter) which were then closed by means of a screwed-nut. The containers were placed on home-made settings (able to accommodate 4 or 8 ampullae in two rows) fastened to a commercial shaking machine (IKA-VIBRAX-VXR). This device generates a horizontal vibrating motion driven by a rotating eccentric gear. Mechanical shakings from 2 to 160 hours were performed. It must be noticed that even after long grinding times, at room temperature, the temperature of the containers had hardly increased (a few degrees at most). So, from a macroscopic point of view, the temperature does not increase during the shaking [12]. Some experiments were carried out with a container equipped with a special screwed-cap which allows to introduce a gas or to create a vacuum inside the ampulla.

We previously describe the mechanical process as observed through transparent Plexiglas caps [12]. To sum it up, “there are almost no shocks, and . . . an overall softened slow rotating (either clockwise or anticlockwise) motion of the balls” was observed. The resulting process can be described by crushing instead of smashing, hence the “low-energy” qualification of the mechanical treatment we perform.

Before and after each treatment, the powders were studied by X-ray diffraction, transmission electron microscopy, IR spectroscopy and granulometry. Some scanning transmission electron microscopy measurements were carried out to perform electron energy loss spectroscopy analyses (EELS).

3. Results

3.1. Powder characterization

3.1.1. X-ray diffraction

Usually, before and after milling, X-ray diffraction patterns (XDP) reveal the classical h-BN phase. The initial powders are well crystallized. As the grinding time increases (60 hours and more), they tend to become ill-crystallized. The diffraction line intensities decrease markedly. In some samples, the diffraction lines become very broad or even disappear into a very broad diffuse feature which means that these samples have become almost or even wholly amorphous.

However, as reported in Table II, after mechanical treatment of BN with or without added water, three samples (hereafter named I-A, II-A, and III-B) underwent unexpected transformations.

Sample I-A is characterized by a possible hexagonal lattice (named H1) with parameters, a_{H1} and c_{H1} , much larger than those of phase h-BN.

Sample II-A was initially composed of an equimolecular mixture of BN (compound A) and water. It was ground for 10 hours. Then, it was left for 2 months inside the closed ampulla. On opening, it was observed that the powder had turned yellow and grey and formed a compact material covered with a hard crust. The container walls were absolutely dry, no trace of moisture could be detected. XDP revealed that narrow diffraction lines were those of the the o-BN structure [5]. Moreover, many broad lines could be indexed according to a primitive cubic lattice (pc) whose parameter a_{pc} is close to parameter c of the hexagonal wurtzite unit cell [8]. Some other lines could not be assigned to any other BN structures. However, another broad diffraction line may correspond to the (111) plane of c-BN.

Sample III-B initially consisted in 2 g of BN with 5 drops of distilled water. Mechanical treatment for 48 hours led to the formation of some unknown phase (or phases): we did not succeed in indexing the corresponding peaks. The (111) diffraction line of the c-BN phase was the most interesting resulting feature. This observation is supported by the emergence in the IR spectrum of milled BN of a shoulder near 1100 cm^{-1} (that is near the positions of IR lines of c-BN [13]) (Fig. 1).

3.1.2. Electron diffraction microscopy

The powders are scattered onto copper grids overcoated with a thin carbon film. Electron diffraction patterns (EDP) are recorded before and after ball-milling by examining particles thin enough. The microscope camera length is determined thanks to the h-BN ring and spot reflections.

a) Before milling, most of the thinner crystals (thickness $<150\text{ nm}$) of A and B powders exhibited the h-BN structure. However, some scattered diffraction spots could be assigned to the o-BN phase [5]. These

TABLE II X-ray diffraction patterns: diffraction lines not correlated to the h-BN phase

| I-BN Type A White- 70 h milling | | | II-BN Type A, grey-yellow 10 h milling under water | | | | III-BN Type B Grey-48 h milling with some water | |
|--|-----|-------|---|-------|---------------------------|-----------------|--|-------|
| New phase: 100% | | | New phases: 50% | | | | New phases: 40% | |
| d_{hkl} | I | hkl | d_{hkl} | shape | $(hkl)_O$ | $(h'k'l')_{pc}$ | d_{hkl} | shape |
| 6.020 | 100 | 11.0 | 6.300 | n | 001 | | 3.055 | vn |
| 5.510 | 80 | 11.1 | 4.190 | b | | 100 | 2.540 | b |
| 3.540 | 80 | 00.4 | 3.800 | n | 210 | | 2.340 | b |
| 3.380 | 80 | 10.4 | 2.950 | b | 102 | 110 | 2.295 | b |
| 2.835 | 60 | 31.1 | 2.680 | b | 310 | | 2.230 | b |
| | | | 2.580 | b | 030 | | 2.090 | n* |
| | | | 2.510 | b | 202 | | 1.910 | b |
| | | | 2.465 | n | 311 | | 1.880 | n |
| | | | 2.440 | b | | 111 | 1.715 | b |
| | | | 2.100 | b | | 200 | 1.595 | b |
| | | | 2.085 | b* | | | 1.465 | b |
| | | | 2.000 | n | 032 | | 1.440 | b |
| | | | 1.965 | n | 411 | | | |
| | | | 1.930 | b | 040 | | | |
| | | | 1.865 | b | | 210 | | |
| | | | 1.845 | n | 023 | | | |
| | | | 1.725 | b | | 211 | | |
| | | | 1.530 | b | | | | |
| | | | 1.520 | b | | | | |
| $a_{H1} = 12.04(4)\text{\AA}$ $c_{H1} = 14.16(4)\text{\AA}$ $= c_r \times 2^{1/2}$ | | | *(111) c-BN | | $a_{pc} = 4.20\text{\AA}$ | | *(111) c-BN | |

b = broad, n = narrow, vn = very narrow.

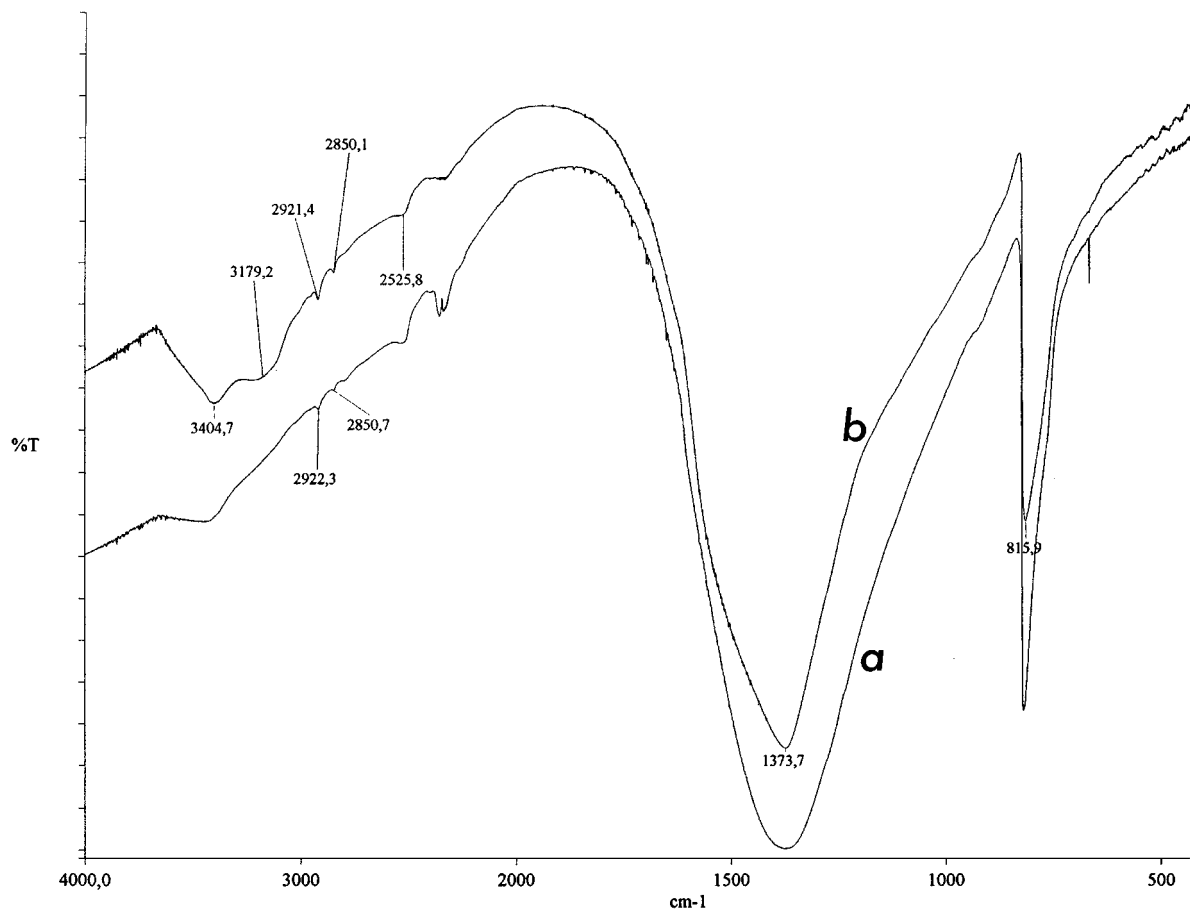


Figure 1 IR spectra of: a) initial BN powder; b) ball-milled BN powder (Note the shoulder on the 1374 cm^{-1} band and the two new bands at ~ 3180 and ~ 3405 cm^{-1}).



Figure 2 Electron diffraction pattern of ball-milled h-BN powder: elliptic rings characteristic of a "turbostratic" material. The first intense elliptic ring relates to the (00.2) crystallographic plane.

spots were more numerous with B-type BN which could be related to the fact that these powders had previously undergone high pressure treatments. Moreover, some other spots and also those scattered by some isolated crystallites exhibiting a six-fold symmetry could be understood in terms of two hexagonal lattices: hexagonal H1 phase (Table II, column I) and H2 with $a_{H2} = 0.666$ nm (it is to be emphasized that $a_{H2} = c_h$; parameter c_{H2} could not be determined, but if the structure of H2 is compact hexagonal, which is a usual hypothesis in TEM studies, $c_{H2} = 1.087$ nm, that is $c_{H2} = 3a_c$). The H2 lattice was never observed through X-ray diffraction.

b) After mechanical treatment, the EDP of the h-BN phase is still preponderant. However, in some cases, the spot rings present the same elliptic configuration (Fig. 2) as "turbostratic" graphite does [14, 15]. This means that the structure of a part of ball-milled hexagonal BN is analogous to that of "turbostratic" graphite with its translational as well as rotational disorder of the (*ab*) planes [15]. Therefore, the mechanical treat-

ment entailed translations and rotations of the h-BN (*ab*) planes with respect to one another. This transformation could be a general property of lamellar product since it was also observed in the case of montmorillonite [16].

Other diffraction features may be observed. A series of diffraction spots can be associated with face centered cubic patterns with different unit-cell parameters (a_F), that of usual c-BN and three other greater values (Table III). Fig. 3 exhibits all the observable (in our experimental d range) diffraction rings of the c-BN structure.

Scattered and isolated spots, or symmetrical spot patterns corresponding to isolated particles lead to interplanar spacings characteristic of the orthorhombic phase reported by Batsanov *et al.* [5]. Such diffractions are observed for all our ball-milling experiments. They are more numerous for powder B.

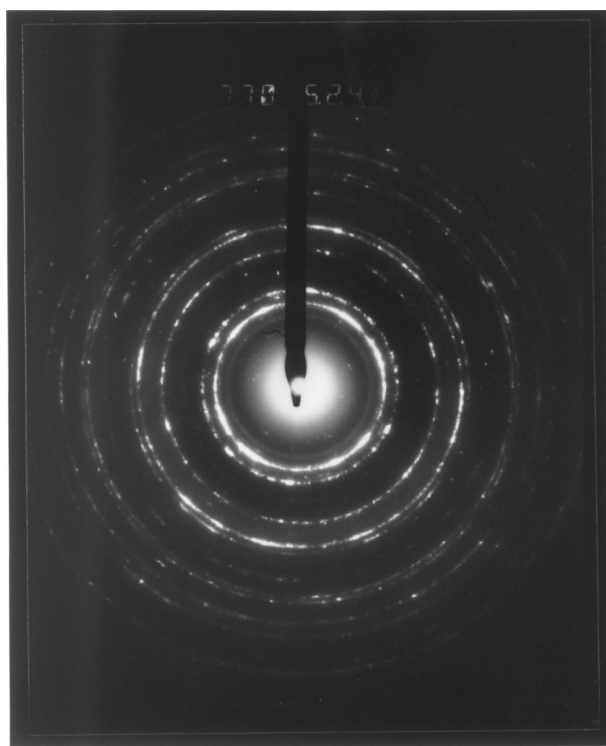


Figure 3 Electron diffraction pattern of ball-milled h-BN powder. The intense ring system, characteristic of the c-BN phase, is defined by the following crystallographic planes: (111), (200), (220), (311), (222), (400), (331), (420), (511) ...

TABLE III Crystallographic structures observed after ball-milling of BN (according to electron diffraction patterns [EDP])

| fcc $a_F/\text{\AA}$ | 6-fold symmetry hep | | Orthorhombic phase | Other structures |
|-----------------------------|---------------------|-----------------------|--|--|
| | $a_H/\text{\AA}$ | $c_H/\text{\AA}$ | | |
| 4.32 = $a_h \times 3^{1/2}$ | 8.58 | 14.00 | Many spots and rings. Many spot patterns exhibit a good correlation between planes and angles. | A great number of other rings and spots could not be correlated to known BN and boron compounds. |
| 4.10 | 6.68 | 10.90 | | |
| 4.05 | 5.22 | 8.52 | | |
| 3.92 | | | | |
| 3.62* | | fcc, $a_F/\text{\AA}$ | | |
| | | 12.12 | | |
| | | 9.45 | | |
| | | 7.38 | | |

*Spot and ring patterns (agglomerates of small crystals) of the c-BN phase.

Some symmetrical patterns cannot be associated with any known phase of BN. For six-fold symmetry patterns, the unit-cell can be either hexagonal or cubic but no other information allows to decide which is true. Finally some scattered and isolated spots could not be assigned to any boron compounds.

Ball-milled powder A was studied by EELS. Powder was dispersed on holey carbon films. The spectra recorded on three different areas thin enough to be studied by this method show that there is no deviation for the plasmon surface (8.3 eV), the plasmon volume (25.8 eV), the B-K edge (between 180 and 225 eV) and the N-K edge (close to 400 eV) with respect to pure BN recordings [17, 18]. This indicates that, from the microscopic point of view, the compound has undergone no electronic change during treatment. Therefore only structural changes during milling should be considered.

3.2. Particle aspects and sizes

3.2.1. Transmission electron microscopy imaging

After ball-milling the crystallites exhibit various shapes: near parallelepipedic figures, very small balls, or small fractured crystals (Fig. 4). High magnification

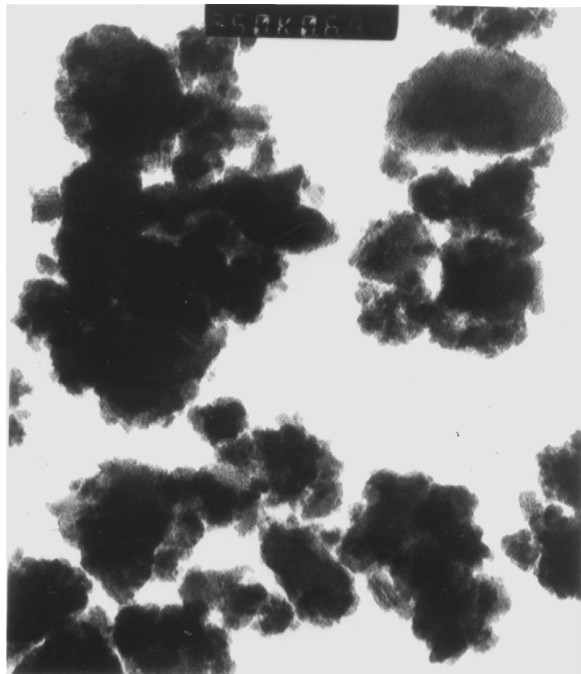


Figure 4 Electron microscopy photograph of ball-milled h-BN powder: thinned and fractured small crystals ($\times 35000$).

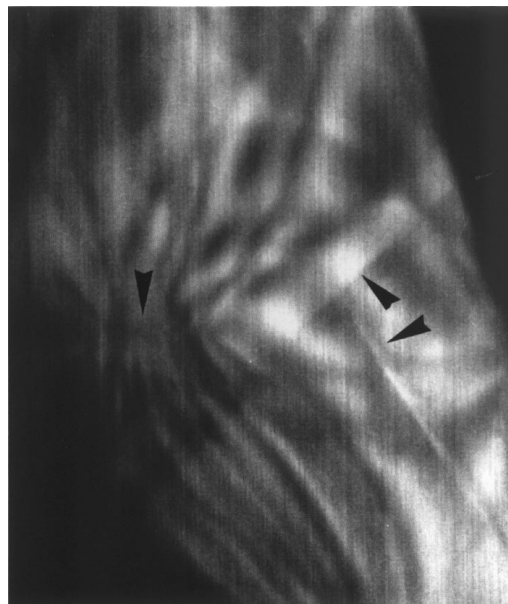


Figure 5 High-resolution electron microscopy of ball-milled h-BN powder: the picture exhibits a pole figure (indicated by an arrow) and two almost perpendicular twin types (indicated by arrows).

images obtained by scanning transmission electron microscopy clearly show the presence of twins and pole figures after grinding (Fig. 5).

3.2.2. Granulometry

The profile populations of the two initial powders were determined by means of a Coulter Laser LS granulometer. The mean grain size of the Aldrich compound was supposed to be $1 \mu\text{m}$ and that of the Grepsy one was supposed to be $2-3 \mu\text{m}$. But powder A was characterized by a medium grain size of $24.5 \mu\text{m}$ and population peaks between 14 and $20 \mu\text{m}$. Powder B exhibited a $12.5 \mu\text{m}$ initial medium size and a large population around $11 \mu\text{m}$. After grinding the medium size of powder A has decreased to $7.5 \mu\text{m}$, its higher peak lying at $10 \mu\text{m}$; a second broad peak is observed between 0.1 and $0.3 \mu\text{m}$ (Table IV). After grinding powder B, the recorded diagram shows three different populations as reported in Table IV. An intense peak lying at about $25 \mu\text{m}$ probably corresponds to aggregates.

Thus, ball-milling BN leads to the usual decrease of grain sizes. Electron microscopy imaging shows clearly that many particles are broken or look like small platelets (Fig. 4). It is to be noticed that, on opening the ampullae just after ball-milling, impalpable smokes come out, indicating the formation of sub-micronic

TABLE IV Grain sizes of BN powders before and after ball-milling

| Population maxima | A-type powder (Claimed size: 1μ) | | | B-type powder (Claimed size: $2-3 \mu$) | | |
|-------------------|---|----------|------------|---|------------|------------|
| | Lower | Medium | Upper | Lower | Medium | Upper |
| Before grinding | — | 11μ | — | — | 20μ | 35μ |
| Ratio % | — | 100 | — | — | 75 | 25 |
| After grinding | 0.3μ | 5μ | $20 \mu^*$ | 0.2μ | $4-10 \mu$ | $25 \mu^*$ |
| Ratio % | ~ 5 | 35 | 60 | 5 | 75 | 20 |

*Due to agglomerates.

powders. Moreover, the ampulla walls are usually covered with tiny particles. This is also the case for the cover inner face which is situated some 6 centimeters above the treated sample. It has been shown previously that there is no convection inside the container [12], which means that many light particles were kicked out by the moving balls.

3.3. Remark: Ammonia-like gas production

As many people who daily use BN, for high pressure experiment for example, and whom we interviewed since then, we were quite unaware of the great sensitivity of BN to water. The results of our experiments forced us to inquire about the influence of water on this compound. It had been noticed [3] that, in cold water, BN was slightly decomposed. In 1911, Vournasos [19] observed that BN was decomposed by hot water with difficulty, and extremely slowly by cold water. In all cases, ammonia was formed. Finally, in 1915, Sborgi [20] reported that 100% pure BN reacted slowly with warm water, and better with boiling water, yielding ammonia in each case. We found no mention of this reaction in literature for the last two decades.

It was also reported that water may be responsible for the formation of either a crystallized hydrated ammonium borate, or of an amorphous ammonium sesquioxiboron [21]; in each case, ammonia emanation was detected. It is now well known that BN can be decomposed at about 1300 K by steam to form B_2O_3 and NH_3 [22], and that BN can be oxidized at about 1100 K [23] or even 800 K according to Montemartini and Losana [24].

Usually after ball-milling and whatever the origin of the BN powders was, there was a strong ammoniated scent at the opening of the container. Sometimes this odor was obtrusive. Sometimes it was a very unpleasant, decay scent (from imines or amides for instance). So far, two experimental series were performed with product A in order to try and determine possible chemical reactions generating ammoniated products. The first series underwent milder treatments:

- i) A powder was stirred inside a container without balls;
- ii) Five drops of water were added to 5 g of BN inside an ampulla which was tightly closed and hold still for two months;
- iii) 2.5 g of BN were shaken gently for 12 hours under a vacuum (~ 10 Pa) inside a container;
- iv) BN powder was first treated at 345 K for 12 hours, then introduced into a container which was put under a vacuum of ~ 1 Pa, then filled up with argon and shaken for 8 hours.
- v) Powder was milled for 120 hours under a vacuum (~ 1 Pa).

For the first three experiments, a slight ammonia-like odor could be detected; for the fourth and fifth ones, it was detectable only after the powder has been slightly stirred or rubbed off from the balls or the walls after opening the container.

The second series was performed in harsher conditions:

- i) Ten water drops were added to powdered BN and the mixture was shaken for 24 hours;
- ii) An excess of boiling water was added to the powder and the mixture was shaken for 12 hours;
- iii) BN powder inside a container was first put under a vacuum (10 Pa) which was then replaced by an argon atmosphere. This time another shaking assembly delivered a violent treatment for about two hours.

In all cases, there was a very strong ammonia-like odor which lasted for several weeks. However, if ammonia was generated, its yield was very low (we could not detect it by means of a very crude chemical method) and our electron diffraction measurements never revealed any crystallite of B_2O_3 which is supposed to be the other product of the reaction of water with BN. Indeed B_2O_3 could have been formed as (or transformed into) an amorphous product, but some crystallites should have subsisted. Therefore, these two results can be viewed as consistent with one another.

Moreover, after milling BN powder under a vacuum, the ammonia-like scent increases for some time after the container has been opened and air enters it. This is reminiscent of the way rare earth metals decompose water vapor at ambient pressure to form hydrides [25]. A possible interpretation is that, in disrupting the BN grains, milling induces the formation of free radicals [26] which are able to decompose water. We performed EPR measurements on BN powder which had been shaken for a few hours under a vacuum (10^{-2} Pa) in a sealed quartz tube, but shaking without steel balls is probably too mild a treatment to induce any visible effect and no free radical could be observed.

On the other hand, if too much water is added to BN powder (50 ml water for 2.5 g BN), milling seems inefficient and leads to a white sludge without any ammonia-like scent.

4. Discussion and conclusions

We just described how ball-milling boron nitride led to the usual decrease in grain sizes and the formation of a wealth of new crystalline phases [27]. The most remarkable are the orthorhombic and the cubic ones which were previously known as very high-stresses [5] and very high-pressure [7] phases, respectively.

It has been found [28] that ball-milling BN facilitates the formation of c-BN through further high temperature-high pressure treatments. For instance, at 7.7 GPa, the formation of c-BN starts at 1523 K with pre-milled h-BN powders, while it starts at 1723 K with non-milled ones. Our results suggest that this could be due to the formation of c-BN nuclei during pre-milling.

The formation of c-BN through milling might be analogous to the synthesis of diamond at room temperature from fullerene C_{60} submitted to high non-hydrostatic pressure [29]. This points out the role of the development of shear stresses in the efficiency of

mechanical treatments for phase transitions and other changes.

The part played by non-hydrostatic stresses is emphasized by the formation of "turbostratic" BN which, revealing rotations of crystallographic (*ab*) planes with respect to one another, implies the shearing action of the milling treatment. This is in agreement with the transmission electron microscopy (TEM) observations of Huang *et al.* [30] according to which, in ball-milled BN, "the shearing angles are quite random and vary from 6° to 26°". They conclude that "the continuous shearing event and the introduction of half Frank loops finally generate an almost turbostratic stacking in h-BN". Chen *et al.* [31] also assigned to turbostratic BN two weak and broadened peaks of the XRD pattern of material resulting from ball-milling of BN, followed by annealing at 1573 K for 10 hours. In such materials, they also observed BN nanotubes. In the present study, no nanotubes were observed, but we cannot say whether a high temperature annealing is necessary to form them or whether a higher TEM magnification is necessary to detect them.

Finally, ball-milling increases the sensitivity of boron nitride to water traces, probably by increasing the surface to volume ratio. The role of water in mechanochemical reactions was recently stressed [32 and references herein]. This should be kept in mind when using BN as a pressure transmitting medium all the more so as stresses usually develop at very high pressures.

Acknowledgements

We thank M. Tancé (Laboratoire de Physique du Solide, Orsay), O. Kaitasov (CSNSM, Orsay), C. Lindecker (IPN, IN2P3, Orsay) and J.P. Michaut (Les Algorithmes, Orsay) for helping with EELS analyses, TEM, granulometry and EPR measurements, respectively.

References

1. S. HORIUCHI, J. Y. HUANG, L. L. HE, J. F. MAO and T. TANIGUCHI, *Phil. Mag. A* **78** (1998) 1065.
2. W. H. BALMAIN, *J. prakt. Chem.* **27** (1842) 422; *Phil. Mag.* **24** (1844) 191.
3. A. STOCK and W. HOLLE, *Ber. Deutch. Chem. Ger.* **41** (1908) 2095.
4. K. SUSA, T. KOBAYASHI and S. TANIGUCHI, *Mater. Res. Bull.* **9** (1974) 1443.

5. S. S. BATSANOV, G. E. BLOKHINA and A. A. DERIBAS, *J. Struct. Chem.* **6** (1965) 209; ICDD-JCPDS, Card no. 18-251.
6. ICDD-JCPDS, Card no. 34-421.
7. *ibid.*, Card no. 25-1033.
8. *ibid.*, Card no. 26-773.
9. T. ISHII, T. SATO, Y. SEKIKAWA and M. IWATA, *J. Cryst. Growth* **52** (1981) 285.
10. S. HORIUCHI, L. L. HE, M. ONODA and M. AKAICHI, *Appl. Phys. Lett.* **68** (1996) 182.
11. A. R. VERMA and P. KRISHNA "Polymorphism and Polytypism in Crystals," (John Wiley and Sons, New York, 1966).
12. H. SZWARC and M. GASGNIER, *J. Solid State Chem.* **136** (1998) 51.
13. S. S. BATSANOV and M. E. V. LAZAREVA, *Zh. Strukt. Khimii* **19** (1978) 753.
14. G. SCHIFFMACHER, H. DEXPERT and P. CARO, *J. Microsc. Spectrosc. Electron.* **5** (1980) 729.
15. J. BISCOE and B. E. WARREN, *J. Appl. Phys.* **13** (1942) 364.
16. J. M. COWLEY and A. GOSWAMI, *Acta Cryst.* **14** (1961) 1071.
17. C. C. AHN and O. L. KRIVANEK, Atlas Electron Energy Loss Spectra, Centre for Solid State Science, ASU, Tempe, AZ 85287.
18. Y. CHEN, J. FITZ GERALD, J. S. WILLIAMS, and S. BULCOCK, *Chem. Phys. Lett.* **299** (1999) 260.
19. A. C. VOURNASOS, *Bull. Soc. Chim.* **IX** (1911) 506.
20. U. SBORGI, *Atti r. ist. Veneto* **74** (1915) 2077.
21. S. ANTOINE, Thèse Université J. Fourier, Grenoble I, 1988.
22. L. VAN MOESER and W. EIDMANN, *Ber. Deutch. Chem. Ger.* **35** (1902) 535.
23. E. PODSZUS, *Z. angew. Chem.* **30** (1917) 156.
24. C. MONTEMARTINI and L. LOSANA, *Notizionio chim. ind.* **1** (1927) 237.
25. M. GASGNIER, J. GHYS, G. SCHIFFMACHER, P. CARO and C. BOULESTEIX, *J. Less-Common Met.* **34** (1974) 131.
26. H. KASHIWAGI and S. ENOMOTO, *Chem. Pharm. Bull.* **30** (1982) 17.
27. D. MICHEL, L. MAZEROLLES, P. BERTHET and E. GAFFET, *Eur. J. Solid State Inorg. Chem.* **32** (1995) 673.
28. S. HORIUCHI, J. Y. HUANG and T. TANIGUCHI, *Electron Microscopy* **2** (1998) 699; Proc. 14th Int. Congress on Electron Microscopy, Cancun, Mexico, 1998.
29. M. NÚÑEZ REGUEIRO, P. MONCEAU and J.-L. HODEAU, *Nature* **355** (1992) 237.
30. J. Y. HUANG, X. B. JIA, H. YASUDA and H. MORI, *Phil. Mag. Lett.* **79** (1999) 217.
31. Y. CHEN, L. T. CHADDERTON, J. FITZ GERALD and J. S. WILLIAMS, *Appl. Phys. Lett.* **74** (1999) 2960.
32. J. TEMUJIN, K. OKADA and K. J. D. MACKENZIE, *J. Solid State Chem.* **138** (1998) 169.

Received 6 May
and accepted 10 December 1999